Organic & Biomolecular Chemistry

Accepted Manuscript

ROYAL SOCIETY OF CHEMISTRY

www.rsc.org/obc

Cite this: DOI: 10.1039/c0xx00000x

www.rsc.org/xxxxxx

ARTICLE TYPE

Multivalent glycosylated nanoparticles for studying carbohydrate-protein interactions

Avijit K. Adak,[a] Hong-Jyune Lin,[a] and Chun-Cheng Lin*[a]

Received (in XXX, XXX) Xth XXXXXXXXX 20XX, Accepted Xth XXXXXXXXX 20XX

DOI: 10.1039/b000000x

Carbohydrates are essential mediators of many important extracellular binding events. Multivalent effects are often required for these binding interactions that are generally weak. Biologically significant carbohydrate-modified nanomaterials are an appealing model system for a systematic investigation of multivalent binding effects. This review seeks to highlight recent striking examples of multivalent glycosylated nanomaterials concentrating on carbohydrate-protein interactions. The specific aim is to provide an overview of various aspects of glyco-nanoparticles in binding assays, targeted therapy, molecular imaging, enzyme activity assay, and bacterium detection.

1. Introduction

Carbohydrates are the most abundant biomolecules and are essential components of surfaces of all cells, including pathogens and viruses. Carbohydrates decorate the surface of cells with a dense layer called glycocalyx. In addition to their uses as energy sources and structural materials, it is becoming clear that glycans (free carbohydrates or carbohydrate fragments of glycoproteins, glycolipids, and proteoglycans) and other glycoconjugates are involved in binding with interacting protein receptors (such as lectins, antibodies, and carbohydrate-processing enzymes) in solution or on cell surfaces.[1] Carbohydrate-protein interactions are critical and guide many biological processes and recognition events, such as intracellular trafficking, cell adhesion, development, cancer metastasis, and immune response.[2-4] Carbohydrates also represent a vital first step in the cycle of infection of hosts by several microbes, including protein toxins, bacteria, viruses, fungi, and parasites.

The interaction between individual carbohydrate ligands and lectins is of low affinity, with dissociation constants typically in the millimolar range.[5] As a result, quantification of these extracellular binding events is difficult. In natural systems, this low affinity is often compensated for by multivalent displays of glycans on (cell) surface scaffolds, such as glycoproteins or glycolipids.[6,7] In multivalent binding, sequential and/or simultaneous multi-point contacts between the clusters of glycans and proteins occur to achieve a measurable association. The multivalent interactions are ubiquitous in biology, enhancing the effective binding affinity (also referred to as avidity) by several orders of magnitude over monovalent carbohydrate-protein interactions to further improve binding specificities.[8]

In nature, most lectins (carbohydrate binding proteins) or receptors are oligomeric proteins with multiple glycan-binding sites. Different strategies have been developed to afford high affinity carbohydrate ligands to measure interactions with these interacting proteins. In the context of multivalent ligand carriers, various well-defined glycosylated nanoscale systems have been developed for the presentation of glycans, including small organic scaffolds, polymers, peptides, proteins, dendrimers, cyclodextrins, liposomes, fullerenes, and nanoparticles.[9-11] In principle, glycopolymers with their inherent flexibility can cover a large area of the cell surface and are therefore able to bridge multiple lectins clustered on a cell surface (i.e., statistical rebinding). However, a small polyvalent scaffold may bind to multiple binding sites of an oligomeric or individual lectin. Conversely, scaffolds based on flat solid surfaces, such as glycoarrays, can be constructed and used to facilitate high-throughput screening of carbohydrate-protein interactions.[12-16] Adjusting the architectural parameters, such as valence, topology, and mode of active ligand positioning, is crucial to maximizing the activities of multivalent glycosylated systems with their binding partners.

Among reported carbohydrate ligand carriers, metallic glyco-nanoparticles (G-NPs) of the glycosylated nanoscale systems occupy a prominent position. G-NPs as scaffolds for three-dimensional polyvalent displays of glycans have several consequences compared to their nano-sized counterparts. Nanoparticles, being small in size, allow a greater contact surface area to improve multivalent interactions. In addition, metallic nanoparticles possess unique electronic, magnetic, and/or optical properties as well as chemical reactivities. Furthermore, the shape, size, and physical properties of NPs can be adjusted selectively, and their surface can accommodate multiple functional groups. These unique features make glycosylated nanoparticles (colloidal gold, binary inorganic nanoparticles, and metal-oxide nanoparticles) particularly well-suited not only for optimizing carbohydrate-mediated interactions but also as attractive systems for numerous applications in biological

research. For example, self-assembly of carbohydrate monolayers on the surface of colloidal gold nanoparticles (commonly referred to as glyco-AuNPs), which were developed in 2001 and are the most studied multivalent nanocarriers.[17,18]

Many excellent reviews have surveyed the methods for the preparation and characterization of G-NPs,[19,20] and, thus, this category is not considered explicitly here. In addition, the preparation and application of polysaccharide-based nanomaterials as carriers for drug delivery have also been covered previously[21] and will not be repeated in this review. Instead, we will focus mainly on specific aspects of metal-based nanoparticles, including semiconductor quantum dots (QDs), iron oxide magnetic nanoparticles (MNPs), and AuNPs covalently conjugated with biologically significant glycans that are essential components of glycoproteins and glycolipids involved in biomolecular recognition events. Particularly, we highlight carbohydrate-protein interactions involving G-NPs in binding assays and demonstrate their potential in targeted drug delivery and diagnostic imaging applications. Finally, we discuss a glyco-AuNP-based assay for determining the activity of an enzyme and briefly outline the advances in label-free methods for the detection of microbial pathogens based on carbohydrate-pathogen interactions.

2. Affinity binding with G-NPs

The detection and characterization of carbohydrate-protein interactions are of crucial importance for the design of more effective carbohydrate-based bioimaging, medical diagnostic, drug delivery, and therapeutic agents for the treatment of diseases and infections. Typical analytical methods for identifying and quantifying carbohydrate-protein interactions of free ligands in solution are NMR spectroscopy, haemagglutination inhibition assay (HAI), X-ray crystallography, enzyme-linked lectin assay (ELLA), isothermal microcalorimetry (ITC), fluorescence microscopy, and surface plasmon resonance (SPR).[11] However, only a few methods have been reported to investigate the quantitative analysis of the binding affinities of G-NPs. Because G-NPs are outfitted with multiple copies of glycans, the binding affinity of free glycans in solution cannot be used as an alternative means for determining the binding affinity between G-NPs and receptors. Depending on the conditions, cooperative binding for enhancing the overall avidity can occur. However, the multivalent binding of G-NPs toward a specific receptor depends strongly on the size of the NP, the number and density of the glycan on the surface, and the variation of the length and flexibility of the spacer within the ligands.

2.1 G-NP model systems for the studies of carbohydrate-mediated interactions

The best-established lectin for carbohydrate-protein interaction is *Concanavalin* A (Con A), known specifically to bind α-D-linked mannose (Man) residues. AuNPs functionalized with monosaccharides (glucose (Glc), galactose (Gal), or Man) were used for quantitative measurement of their binding affinities with Con A (Figure 1).[22] A competition binding assay was carried out using SPR to establish equilibria between an α-D-mannoside-coated SPR sensor chip, Con A, and Man-AuNPs. The inhibition constant (K_i) was found to be 2.3 nM, over 6 orders of magnitude higher in affinity compared to the free αMeMan (α-D-methyl-mannopyranoside) with Con A in solution. In addition, larger glyco-AuNPs with a diameter (d) of 20 nm exhibited higher relative inhibition potency (RIP) than smaller nanoparticles (d ~6 nm), in support of the geometric requirements for the Con A binding sites. Additional studies have emphasized the affinity between a number of monovalent Man-functionalized nanoparticles and Con A lectin, including dynamic light scattering (DLS),[23] quartz crystal microbalance (QCM),[24] and ITC.[25] Based on the energetics of these interactions, the apparent dissociation constants (K_d) of G-NP-lectin interactions are mostly in the nanomolar range. An alternative method or model for K_d evaluation using protein-conjugated iron oxide/gold core/shell nanoparticles exposed to interaction with carbohydrate ligands on a glycan microarray was also discussed.[26] The carbohydrate-protein interaction was further amplified by using an external magnetic field, and the binding signal was visualized and quantified by a silver staining solution. On this platform, the apparent K_d for the Con A-coated MNPs to the Man-coated array was determined to be 66 nM.

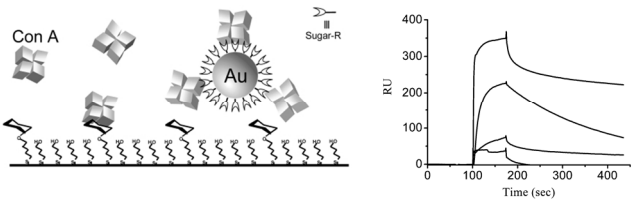

Figure 1. Schematic representation of interaction between glyco-AuNPs and Con A lectin on a SPR chip used in the competition assays (*left*). Inhibition of 0.5 μM Con A binding to the chip by Man-AuNP (*right*). A set of inhibition curves for 0, 0.175, 0.5 and 1.0 μM Man-AuNPs (*from top to bottom*). Reproduced from ref. 22 with permission from The Royal Society of Chemistry.

One common strategy to modulate ligand affinity on NPs to lectin is to vary the length and flexibility of the spacer between the ligand and the NP surface. Yan and co-workers introduced a photo-induced coupling reaction for attaching various unprotected mono-, oligo-, and polysaccharides, such as Man, Glc, di-Man, tri-Man, maltopentose, and dextran, covalently to the AuNP surface using perfluorophenylazides as photoactivatable reagents that contain different linker types and lengths.[27] The fluorescence competition assay was used to measure the binding affinity of these glyco-AuNPs with Con A. The K_d of a monovalent Man-conjugated AuNP containing an amphiphilic linker was determined to be 0.43 nM, an over 6 orders of magnitude higher affinity with respect to αMeMan. Photocoupling provides efficient glycoconjugation and retains the recognition abilities of saccharides to lectins without the need to specifically control the stereochemistry of immobilization. Thus, this protocol may be especially suitable for conjugating oligo- and polysaccharides on NPs.

The length of the spacer is also a major factor affecting the binding affinity of G-NPs to interacting lectins. AuNPs with a d of 20 nm, which had a relative long spacer, were found to be a considerably more potent inhibitor for the B-subunits of Shiga-like toxin I (B-Slt).[28] In this study, multivalent interactions between toxin Slt-I and AuNPs coated with globotriose (Galα1,4Galβ1,4Glcβ- or Gb3, also known as P^k antigen or CD77) ligand were examined, and the affinity was observed to be

a function of particle size and spacer length. SPR measurements revealed that P^k-AuNPs (d ~4 and 20 nm) containing *ca.* 60 and 1970 Gb3 moieties on the surface, respectively, show varying relative inhibition potency per Gb3 ligand on the NP surface from ~1300 for the smallest particles to ~228,000 for the larger particles. The strongest inhibition potency shown by larger nanoparticle (d ~20 nm) may be due to the higher radius of curvature of the gold surface, which can provide intimate contact more efficiently with the binding sites of the B-Slt (Figure 2). Conversely, small curvature of the ligand surface allows insufficient contact and was deduced to be greatly affected by the spacer length for smaller nanoparticles (d ~4 nm).

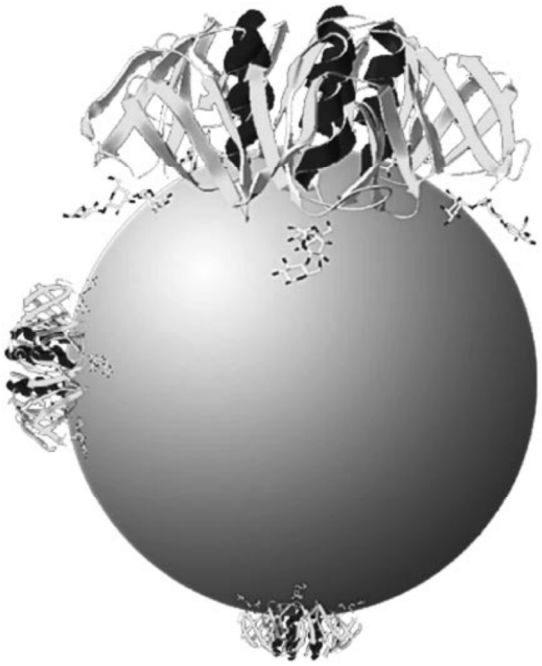

Figure 2. Relative size of the Gb3-functionalized AuNPs and B-Slt. 4-P^k-s-AuNP (*top*), 13-P^k-s-AuNP (*left*), and 20-P^k-s-AuNP (*bottom*) interacting with a B-Slt pentamer. Reproduced with permission from ref. 28. Copyright 2008 John Wiley & Sons.

The anticipated advantage of using AuNPs as the nanocarrier to mimic the patch of the Gb3 on the cell surface can be adapted for intervening in the selective inhibition of different variants of pathogenic Shiga toxins (Stxs). In this regard, AuNPs coated with Gb3 and its analog, with replacement of the terminal Gal as *N*-acetylgalactosamine (GalNAc), respectively, were prepared and used to compete in binding with these toxins.[29] The glyco-AuNPs were found to be nontoxic to the Vero cells (monkey kidney cell line), and cells were protected in a dose-dependent manner from Stx-mediated toxicity. The AuNPs coated with the Gb3 analog were determined to be selective for more toxic Stx2. In addition, this study also showed that a 75% Gb3 coverage on the NP surface decreased the inhibitory threshold of Stx1 10-fold in comparison with 100% Gb3-coated AuNPs.

Glyco-AuNPs were also utilized for selective and quantitative detection of carbohydrate-binding proteins, such as RCA_{120} (*Ricinus communis* agglutinin 120),[18,30] cholera toxin,[31] and human influenza virus,[32] but with no indication of the multivalency effect provided by the glyco-AuNPs. The glycan density (presentation) on designed multifunctional nanomaterial systems plays an important role in effecting G-NP affinities and has been addressed in a recent review.[33] Displaying multiple carbohydrate ligands on NPs has the additional advantage of creating a high local concentration of binding molecules. As a result, the binding equilibrium between a receptor molecule and surface-bound carbohydrates favors the formation of more ligand-receptor pairs. Similar to the concept of carbohydrate microarrays, a new type of 3D microarray platform based on G-NPs has recently been reported to further improve the glycan-lectin interactions.[34] Several Man-NPs were immobilized on the surface upon light activation, and fluorescently labeled Con A lectin was used to probe the affinity of the surface bound G-NPs. The result indicated that G-NP microarrays displayed higher fluorescence signals than 2D glycoarrays.

QDs are nanometer-sized fluorescent semiconductors that exhibit narrow size-dependent emission with high quantum yield and low photobleaching.[35] Carbohydrate-encapsulated QDs (G-QDs) are also useful nano-glycoprobes for investigating carbohydrate-protein interaction and detection of lectins, but only a few studies have been reported.[36-38] G-QDs have been utilized for detecting binding specificities of sugars using a lectin-coated gold microarray.[39] GalNAc-specific lectin and peanut agglutinin (PNA) were covalently immobilized on the gold slide surface, and the electrochemical readout was defined as the detection platform for the binding event to its natural ligand, GalNAc coated to CdS QDs, that occurred. The detection sensitivity of PNA at 0.1 μM could reliably be achieved using this method. In addition, CdSe/ZnS QDs functionalized with Lac, melibiose, and maltotriose with d ~4 nm that displayed between 2 and 35 sugar moieties were utilized for the detection specificity and efficiency with Con A by monitoring light scattered at 600 nm.[40] The results showed a detection limit of 100 nM by specific Con A-induced aggregation of maltotriose-QDs.

Because blocking the glycan binding proteins or lectins may be beneficial for the treatment of various disease states, many inhibitors and antagonists with multivalency have been designed and prepared with various architectures, including G-NPs.[41] Following this scenario, cellular labelling and targeted imaging could be achieved by magnetic and fluorescence nanoprobes. In the following sections, the most commendable examples of G-NPs in the applications of labelling, imaging, and antiadhesion therapy will be discussed.

3. G-NP-based biodiagnostics, drug delivery, and assay of enzyme activity

3.1 G-NPs as multivalent probes for *in vitro* and *in vivo* imaging

Although metal-based saccharide-conjugated nanoparticles, such as AuNPs, semiconductor QDs, and metal-oxide nanoparticles, have been prepared and effectively exploited to date, only a few examples[42-44] have been reported for the use of G-NPs in biomedical imaging applications such as magnetic resonance imaging (MRI). Because the preparation of glyco-AuNPs as imaging probes requires additional synthetic modifications of the carbohydrate shell, enormous efforts have been devoted toward the development of robust glyco-AuNPs with magnetic and

luminescent properties.[45,46] For example, a gadolinium (Gd)-based paramagnetic contrast agent (positive T_1) was synthesized by introducing chelated Gd(III) agents into the organic shell of the AuNP that had been decorated with different carbohydrates (Glc, Gal, or Lac).[45] As shown in Figure 3, Glc was selected as the surface decorated monosaccharide to help G-NPs cross the blood-brain barrier (BBB) in glioma mice (generated with GL261 tumor cells). The preliminary *in vivo* imaging showed that Gd (III) Glc-AuNPs provide ~2-5-fold higher longitudinal relaxation values compared to Dotarem® used clinically. In contrast, Gd (III) Lac-AuNPs were found to enhance contrast outside the brain but did not reach the tumor, possibly because of asialoglycoprotein receptor (ASGP-R)-mediated liver uptake, resulting in the less effective *in vivo* contrast enhancement of Lac-AuNPs in the brain tumor. Very recently, a BBB-permeable neuropeptide, Tyr-Gly-Gly-Phe-Leu (Enkephalin, Enk) and a cyclic chelator (1,4,7-triazacyclononane-1,4,7-triacetic acid, NOTA) containing ^{68}Ga(III) as positron emitter were fabricated onto Glu-coated AuNPs for the assessment of *in vivo* biodistribution and BBB-permeation.[47] This study indicated that Lip-Enk-G-NP (d ~2 nm) containing a lipoic acid (Lip) linker provides *ca.* 2.5-fold higher uptake values in the brain of animals when compared to a nontargeted control G-NP, Lip-G-NP.

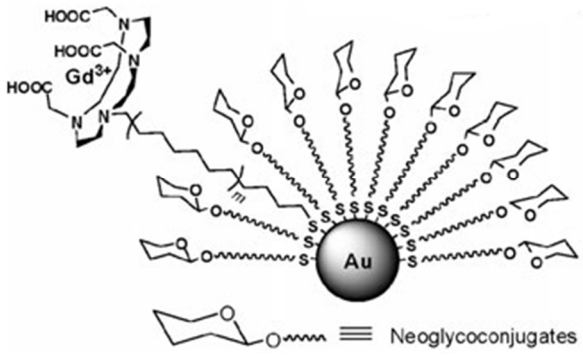

Figure 3. A paramagnetic G-NP as MRI contrast agent. The DO3A-Gd complex serves as T1-contrast agent for MRI imaging. Reproduced from ref. 45 with permission from The Royal Society of Chemistry.

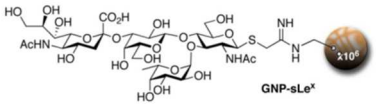

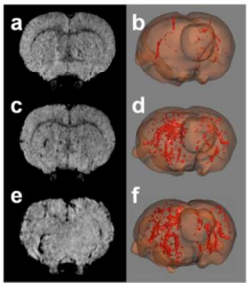

Figure 4. Sialyl-Lewis X (sLeX)-functionalized MRI-active magnetic G-NPs for E-selectin, and their presymptomatic in vivo imaging of brain diseases. Selected images taken from the T2*-weighted 3D datasets (a, c, and e) and 3D reconstructions of the accumulation of contrast agent (b, d, and f) reveal that G-NP-sLex enables clear detection of lesions in clinically-relevant models of multiple sclerosis (c and d) and stroke (e and f) in contrast to unfunctionalized control-NP (a and b). Reprinted with permission from ref. 42. Copyright (2009) National Academy of sciences.

With respect to presymptomatic *in vivo* imaging of brain diseases, MRI-active magnetic G-NPs functionalized with sialyl-Lewis X (sLe^X), which specifically recognizes carbohydrate-binding transmembrane protein (E-selectin, CD62E), have been designed.[42] Several glycans were chemoselectively attached on the amine-functionalized magnetic-NP (MNP) surface through the formation of an amidine linkage using a 'masked' *S*-cyanomethyl group at the linker of glycans to provide high conjugation yields with 10^5 to 10^7 copies of glycans per NP. The magnetic G-NPs have allowed direct detection of an activated endothelial marker by means of MRI (Figure 4). In addition to amidine linkage, amide bond formation was also employed to introduce amine-terminated sLe^X onto the iron oxide MNP surface as vasculature targeting motifs for endothelial inflammation.[48]

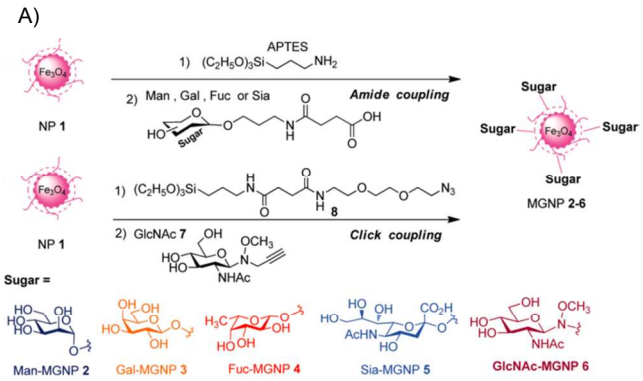

Figure 5. Synthesis of magnetic glyco-NPs via amide coupling and click chemistry (A). Magnetic Gal-NPs was used to distinguish malignant and normal breast cancer cells based on MRI response signatures (B). Significant differences in binding with MGNPs were observed, thus differentiating these cell lines. Reprinted with permission from ref. 43. Copyright (2010) American Chemical Society.

To use magnetic G-NPs as target-specific MRI agents, the iron-oxide MNPs were functionalized with five different monosaccharides, Man, Gal, fucose (Fuc), sialic acid (Sia), and N-acetylglucosamine (GlcNAc) (Figure 5A).[43] The magnetic G-NPs were used not only to detect and differentiate cancer cells but also to quantitatively measure the carbohydrate binding ability by MRI. When magnetic G-NPs were incubated with cancer cells, cells were aggregated and produced a shorter T2 (transverse relaxation time) and darkened MRI images. One

notable advantage of this method is the differentiation of cancer cells in the presence of normal cells using MRI response as a molecular signature despite the use of only a simple monosaccharide as the targeting ligand. As an example, breast cancer MCF-7/Adr-res cells exhibit a significantly larger T2 change after binding to magnetic Gal-NPs compared to the T2 change of normal breast endothelial cell 184B5 (Figure 5B). This technique has been used to distinguish 10 cell lines by LDA (linear discrimination analysis) based on their respective MRI signatures.

Fluorescent MNPs were also demonstrated to be ideal non-invasive contrast agents for biological imaging due to the presence of dual fluorescent and magnetic properties. For example, silica-coated MNPs decorated with Gal were used to target specific cancer cells.[49] To generate a fluorescent MNP with target-specific ligands, a small amount (5%) of fluorescent dye, Cy3, and triantennary dendritic galactoside (T-Gal) ligands were incorporated on the MNP surface. The multifunctional MNPs interact with ASGP-R on the cell surface of liver cancer cells (HepG2 cell) and trigger subsequent internalization via receptor-mediated endocytosis. In addition, the pre-assembled tri-Gal ligands on the nanoparticle surface were found to be crucial to the avidity of magnetic G-NPs to cancer cells.

Carbohydrate-functionalized binary inorganic NPs, such as G-QDs, have also been developed as probes for *in vivo* optical imaging and for labelling cells. For *in vitro* labelling of cells, Man and GlcNAc were conjugated with CdSe/ZnS core/shell QDs and then used for labelling sperm obtained from pigs, mice, and sea-urchins.[50] Analysis by fluorescence imaging revealed that Man-QDs spread over the whole sperm body, while GlcNAc-QDs specifically accumulated only at the sperm heads, which was attributed to a different distribution of receptors to Man and GlcNAc. A similar CdSe/ZnS core/shell G-QD functionalized with Gal residues has been examined for specific cellular uptake of QDs by ASGP-R-mediated endocytosis.[51] Fluorescence imaging examination after 3 h of incubation indicated preferential binding and uptake of Gal-QDs by lung cancer cells compared to an unfunctionalized QD. In addition, receptor-mediated uptake of mannosylated PEG_{2000} QDs have been suggested for the labelling of macrophages.[52]

For *in vivo* optical imaging of G-QDs, different monosaccharide (Man-, Gal-, or D-galactosamine (GalN))-capped PEGylated QDs were synthesized to study the specific carbohydrate-protein interactions.[53] When G-QDs were injected into mice, both Man- and GalN-encapsulated QDs (note: Gal-QD was not tested) were taken up by the liver after two hours as controls (unfunctionalized PEGylated-QDs) showed only an unspecific pattern. These results determined that the Man receptor and ASGP-R are responsible for mediating specific binding of G-QDs in the liver. A recent study exploited enzymatic sugar elongation on phosphorylcholine (PC)-stabilized QDs as a platform to generate multifunctional high complex glycan (sialyl LacNAc and Le^X) QDs.[54] After intravenous injection of G-QDs into a mouse, *in vivo* near-infrared fluorescence imaging showed that only sialylated-QDs were still retained in the whole body up to 2 h (longitudinal study), while other G-QDs examined circulated and accumulated in the liver within 5-10 min.

3.2 Glycosylated nanosystems for target-specific delivery

Novel drug delivery systems and nanomedicines continue to emerge in the laboratory and show a clinical impact.[55] Greater targeting selectivity and better delivery efficiency are two of the most important characteristics in the development of therapeutic agents for enhancing bioavailability while avoiding toxicity to normal cells. For example, paclitaxel (PTX), one of the most popular chemotherapeutic agents, has been conjugated covalently to AuNPs[56,57] to increase the intracellular concentration of the drug in tumor cells. However, this NP-based assembly is lacking the targeting ligand on the NP surface. The surfaces of NPs can be engineered with synthetic control to load more targeting ligand and therapeutic agents to overcome limitations such as nonspecific delivery and inadequate drug concentration in a cell. Lin and co-workers developed a stepwise orthogonal click approach to effectively assemble a targeting ligand, T-Gal, and PTX onto a Cy3 doped-silica NP, denoted as TGal-PTX @$Cy3SiO_2$NPs (Figure 6).[58] The low aqueous solubility and nonspecificity of the free PTX were improved greatly by the introduction of the hydrophilic T-Gal ligand onto fluorescent NPs with high PTX loading (0.68 ± 0.09 PTX/nm^2). Cytotoxicity assays indicated that PTX on the NP retains its function and shows a dose-dependent killing effect. Recently, a similar dually-functionalized AuNP appended with Lac as targeting ligand for lectin human galectin-3 (Gal-3) and β-cyclodextrin (β-CD) for encapsulating anticancer drug methotrexate (MTX) is reported.[59] The drug carrying capability of the NP was measured by UV-vis spectroscopy. However, no estimation on the loading amount was provided.

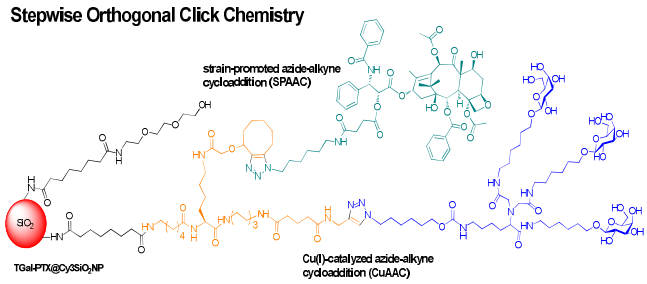

Figure 6. A fluorescent silica nanoparticle (TGal-PTX@$Cy3SiO_2$NP) consisting of a targeting ligand and a chemotherapeutic agent for selective targeting of cancer cells. Reprinted with permission from ref. 58. Copyright (2013) American Chemical Society.

Boron neutron capture therapy (BNCT) is a binary treatment especially suited to radio-resistant and highly invasive tumors.[60] The clinical success of BNCT depends mainly on internalizing a large number of boron-10 (^{10}B) nuclei (approximately 15-30 μg of B per g of tumor or 10^9 atoms of ^{10}B per tumor cell) into the target cells. To achieve target-specific delivery of BNCT reagents, T-Gal-functionalized carborane,[61] an icosahedral cage containing several B atoms, or T-Gal conjugated mesoporous silica NPs (MSNs) consisting of carborane units[62] were developed. The presence of T-Gal ligands on a multifunctional MSN surface increases the hydrophilicity and enhances the BNCT effect by targeting ASGP-Rs on the HepG2 cell surface. In *in vitro* test, T-Gal-MSN shows 50-fold higher efficiency for

delivering B atoms into a cell compared to sodium borocaptate (BSH),[61] providing an excellent BNCT effect upon neutron irradiation.

3.3. Glyco-AuNPs in agglutination-based enzyme activity analysis

AuNPs possess unique optical properties, in particular a strong surface plasmon resonance, which can be orders of magnitude higher than the optical properties of common fluorescence dyes.[63] These features, together with ease of synthesis and exceptional stability in physiological media, make them particularly suitable for applications in imaging, biological sensing, and medicine.[63,64] The structures of AuNPs can also be engineered to generate a useful platform in bioanalytical applications. Although AuNP-based aggregations have been developed in assaying target proteins,[64] for the enzyme activity assay, most of the studies were focused on the hydrolytic activities of enzymes.[65-67] A recent study has suggested that a visual screening of the bond-forming activity of a glycosyltransferase can be conducted by a colorimetric assay based on the aggregation of AuNPs. In this regard, ganglioside GD3-tetrasaccharide-functionalized AuNPs (GD3-AuNPs) were used as a substrate for enzymatic sialylation using α-2,8-polysialyltransferase (α-2,8-PST), an enzyme that is primarily responsible for the biosynthesis of polysialic acid (PSA) (Figure 7).[68] A catalytically inactive endosialidase (EndoNF-DM) was used to cross link the polysialylated nanoparticles to induce aggregation and a simultaneous change of color compared to the control (GD3-AuNPs) nanoparticles without α-2,8-PST treatment. A similar concept can be applied on assaying the activities of glycosyltransferases and finding inhibitors of glycosyltransferases.

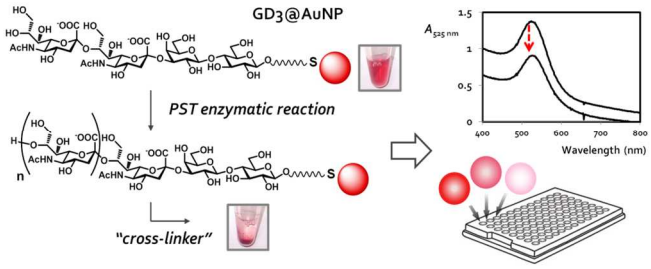

Figure 7. A glyco-AuNP based colorimetric assay for specific bond-forming activities of enzymes. Reproduced from ref. 68 with permission from The Royal Society of Chemistry.

4. G-NPs and glycosylated surfaces for microbial adhesion and detection

4.1 G-NPs and glycosylated surfaces for microbial adhesion and detection

The adhesion of bacteria to glycosylated surfaces and cells is facilitated mostly by the multiple filamentous protein appendages called fimbriae or pili projecting from the surface of bacteria. The lectin FimH is known to mediate adhesion in an α-D-Man-specific manner and is positioned at the tips of type 1 fimbriae in *E. coli*. Because adhesion protein FimH is well characterized, most of the studies have focused on the capture of the type 1 fimbriated strain of *E. coli*. A seminal work dealing with glyco-AuNPs as a bio-label for microbial pathogens was reported in 2002.[69] The specific binding of the Man-AuNPs to the FimH of *E. coli* strain ORN178, which expresses the wild-type type 1 pili, was directly visualized by transmission electron microscopy (TEM). A selective binding was demonstrated by using a *fimH*-deficient strain (ORN208) that failed to mediate the Man-specific adhesion to the nanoparticle surfaces. From this work on, many others have prepared several glyco-AuNPs and applied them as nanoprobes to label bacteria and viruses in biological systems.[20] A well-studied example is the multivalent high-affinity binding of sialic acid-functionalized AuNPs to the viral fusion protein hemagglutinin (HA) of influenza A virus.[70] As shown by the TEM image (Figure 8), multiple binding (three effective bonds) of individual larger AuNPs (d ~14 nm) to viral HAs could be observed. However, smaller-sized nanoparticles (d ~2 nm) simply attached on the viral envelope as black dots, most likely because their small size kept them away from binding several HAs at once. This study also illustrates that sialylated-AuNPs are potent inhibitors of influenza virus infection.

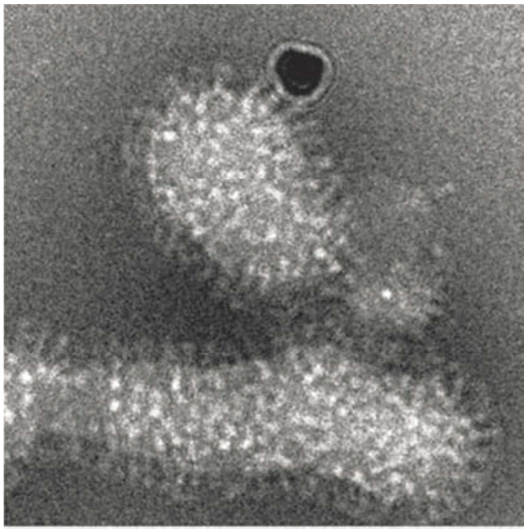

Figure 8. Influenza A virions after 60 min incubation with sialylated-AuNPs (d = 14 nm). The multiple attachment of particles to virions is clearly visible. Closer inspection suggests that several HA trimers are involved in the particle binding. Reproduced with permission from ref. 70. Copyright (2010) John Wiley & Sons.

Glyco-MNPs have also been applied to the detection of bacteria.[71,72] Similar to Man-AuNPs,[22] the Man-MNPs showed ~200-fold higher affinity to Con A in comparison with monomeric Man.[71] The high avidity of Man-MNPs was utilized for specific binding of FimH protein in *E. coli* ORN178 to rapidly detect bacteria with a concentration of 10^4 cells/mL. The use of glycan-based affinity capture would be particularly challenging because different strains of bacteria may have a similar affinity to the same glycan ligands. In a model study, three different *E. coli* strains (ORN178, ORN208, and an environmental strain) were tested for strain-specific binding based on the response patterns to Man-MNPs and Gal-MNPs. A similar strain-specific separation and differentiation of fluorescently labelled *E. coli* ORN178 and ORN208 strains using Man-MNPs has been described by

fluorescence microscopy.[73] In addition to the use for lectin detection, G-QDs have also been employed in the selective detection of bacteria.[74] QDs coated with Man ligand induced the formation of luminescent aggregates, which led to the detection of *E. coli* strain ORN178 at concentrations as low as 10^4 cells/mL. In addition, galabiose (Galα1,4Gal)-conjugated submicrometer particles were employed to detect *Streptococcus suis*, a Gram-positive pathogen that binds specifically to glycans with a non-reducing end Galα1,4Gal.[75] Both mono- and tetravalent biotinylated galabiose derivatives were conjugated to streptavidin-coated magnetic particles with a submicrometer dimension (d ~250 nm) and interrogated with *S. suis*. A standard luminescence-based adenosine triphosphate (ATP) assay revealed that the smaller size of the glyco-particles (d ~250 nm) permitted bacterial detection, but larger particles (d ~10 μm) failed to recognize and bind to bacteria. This difference in binding affinity provided additional support in favor of a large surface area also being an important factor for the multivalent effect.

Glycosylated nanomaterials have also found use in the detection of pathogenic bacteria in a sandwich-type assay. In a proof-of-concept study, nanodiamonds (NDs) were easily functionalized with Man-derivatives by thiolene reactions or amide bond formation, and the glyco-NDs were used to form adhesive films between two bacterial layers.[76] In such a sandwich-type assay (Figure 9), a sigmoidal dose-responsive curve of glyco-NDs to GFP-tagged bacteria was obtained, indicating specific lectin-carbohydrate mediated interactions because a negative control experiment produced no apparent fluorescence signal. In an optimal setup, these glyco-NDs were also found to efficiently remove more than 90% of the bacteria from contaminated solutions by filtration through carbohydrate-mediated precipitation.

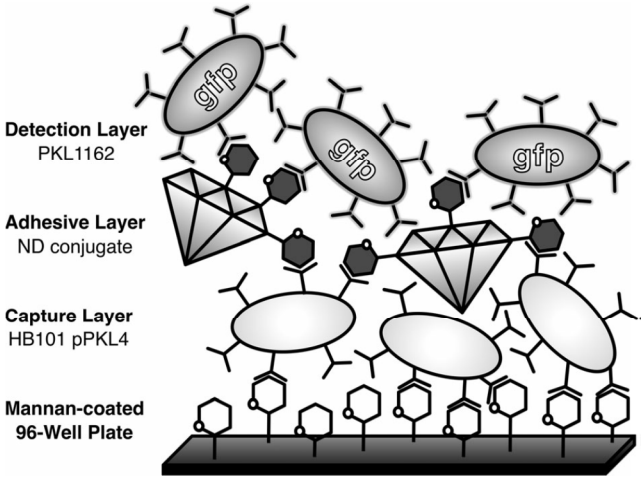

Figure 9. Setup of the sandwich assay: type 1 fimbriated *E. coli* (HB101 pPKL4) are immobilized onto polysaccharide (mannan)-coated microtiter plates. Then, serial dilutions of ND conjugates are applied; this leads to an adhesive layer, to which fluorescent type 1 fimbriated *E. coli* (PKL1162) can adhere as the detection layer. Thus, fluorescence intensity is correlated with the adhesive properties of the applied ND conjugates. Reproduced with permission from ref. 76. Copyright (2012) John Wiley & Sons.

Carbohydrate-protein interactions between pathogens and the host cells facilitate pathogenic infections. Carbohydrate ligands with multivalent presented ligands can serve as effective inhibitors to disrupt the initial step of infections. G-NPs with various glycan coverage and topology have been designed as high affinity carbohydrate-based anti-adhesive agents. As an illustration, AuNPs were functionalized with varying Gal densities (17%, 33%, 80%, 90%, and 100%), and their binding interactions with *Pseudomonas aeruginosa* lectin PA-IL (LecA) were measured by HAIs.[77] The glyco-AuNPs with a 100% Gal density were determined to be the most effective inhibitor, with a K_d of 50 nM, representing a 3000-fold binding affinity enhancement compared to monovalent Gal (K_a = 3.4 x 10^4 M^{-1}). With respect to the effect of ligand topology on the surface, the preparation of nanosized carriers using various glycan structures remains an area in progress.[78,79] In the example below, Man-AuNPs were tested for the inhibition of dendritic cell-specific intracellular adhesion molecule-3-grabbing non-integrin (DC-SIGN) binding to the human immunodeficiency virus (HIV-1) envelope glycoprotein gp120 using the SPR assay.[78] Multiple copies of partial structures derived from the *N*-linked high-Man type glycans of viral gp120, such as di-, tri-, tetra-, penta-, and heptamannosides, were decorated on the surface of AuNPs with varying densities (10, 50 and 100%). The SPR binding results showed that a G-NP with 50% Manα1-2Manα-ligand on the surface provides a remarkable inhibition with ~20,000-fold higher activity than monomeric mannoside. This study indicated that glyco-AuNPs could function as an anti-adhesive and may resist attachment of HIV to DC-SIGN expressing cells. In addition, a recent study proposed that glyco-AuNPs presenting galactofuranose (Gal*f*), a five-membered ring form of Gal, mediate the binding of human monocyte derived DCs through interaction with lectin, DC-SIGN.[80]

4.2 Functional slide surfaces for cellular, bacterial, and pathogenic adhesion

Employing glycosylated micropatterned surfaces for recognizing cells offers the advantage of the multivalent display of carbohydrate ligands to mimic binding interactions at cell-cell interfaces. Mannosylated glycoarrays were applied to capture *E. coli* strain ORN178, and the presence of the bacterium was detected by fluorescence and bright-field microscopy.[81] In this platform, fluorescent bacteria (ORN178) were specifically detected with concentrations down to 10^5-10^6 cfu/mL, raising the opportunities to use suitably designed functional surfaces for the early detection of human pathogens.[82,83]

Microbial pathogens are constantly mutating and can consequently produce strains capable of evading detectors that depend on the recognition of nonfunctional surface antigens. Recently, an alternative to antibody-based capture of bacterial pathogens exploiting the native capacity of the pathogen to recognize and bind glycans on the surface of the host cell was proposed.[84,85] The recognition of such ligands is deemed to be "immutable" because pathogen virulence often correlates with glycan binding. In the example below, a glass slide was patterned with a trisaccharide, GalNAc(β1→4)Gal(β1→4)Glc, a substructure of asialo-GM2 that shows a high affinity with opportunistic pathogens implicated in respiratory tract infections, such as Gram-negative *P. aeruginosa* and multi-drug resistant

Staphylococcus aureus (Figure 10).[85] Bacterial concentrations as low as 10^3 cfu/mL can be detected by optical darkfield imaging for 30 min on ligand-patterned substrates. In addition, simultaneous screening of the pathogenic *Vibrio cholerae,* responsible for the human disease cholera, on the trisaccharide-patterned chip produced no apparent binding, highlighting selectivity among different bacterial types for the glycan structure. The authors introduced fast Fourier transform (FFT) analysis as a label-free readout, providing sensitive signals with a limit of detection well below the threshold of visual inspection. The work demonstrated the possibilities of such platforms as rapid, fault-tolerant, and low cost alternative screening methods for multiplex pathogen detection.

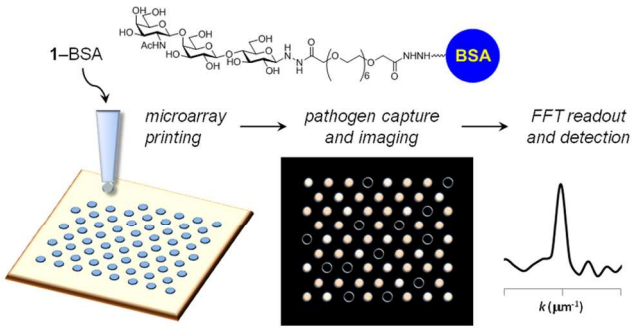

Figure 10. Immutable ligand arrays for label-free detection of bacterial pathogens. *Left*, inkjet deposition of neoglycoprotein onto activated glass substrates (with the option of generating multiple periodicities); *middle*, microarray exposed to pathogens, with label-free imaging of bacteria under darkfield conditions; *right*, image processing by FFT reveals emergence of a signature peak in Fourier space, corresponding to the periodicity of the capture array. Reprinted with permission from ref. 85. Copyright (2013) American Chemical Society.

Conclusions

The design of high-affinity multivalent lectin ligands is crucial for the generation of drugs for therapeutic and biodiagnostic applications. G-NPs are attractive scaffolds because they constitute a good bio-mimetic model of multivalent presentation of glycans and show tremendous enhancement of the overall avidity compared to monovalent binding events. Many different aspects of potency enhancement in some of the recent anti-adhesive, bioimaging, and target-specific delivery systems have been discussed using NPs modified with biologically relevant carbohydrates. This review has also attempted to generate interest in the use of glyco-AuNPs for assaying specific bond-forming activities of glycosyltransferases and functional surfaces for the label-free detection of microbial pathogens with an option for multiplexing. However, for the rational design of targeting G-NPs, the influences of the ligand structure, its surface density and a suitable spacing to bridge the binding sites need to be optimized further based on the knowledge of the targeted protein structure. Current nanocarriers used clinically for therapeutic drugs, including liposomes and polymeric nanoparticles, have limitations, such as low cellular uptake and low diffusion rate into tumors. By contrast, multifunctional G-NPs offer a viable alternative to such systems by selectively targeting cell types with lower intrinsic toxicity toward the environment and living systems. Furthermore, multifunctionality of the glycosylated nanomaterial systems could readily be obtained by simultaneous incorporation of a variety of ligands, fluorescent dyes, and magnetic elements. We anticipate that the methods and materials developed will enable the design of sensitive diagnostic tools and provide more efficacious carbohydrate-based polyvalent therapeutics in nanomedicine.

Acknowledgments

We gratefully acknowledge the financial support from the National Tsing Hua University and the Ministry of Science and Technology of Taiwan.

Notes and references

[a]*Department of Chemistry, National Tsing Hua University, Hsinchu 30013, Taiwan. E-mail:* cclin66@mx.nthu.edu.tw*; Tel: +886 3 5753147; Fax: +886 3 5711082.*

1 H. Lis and N. Sharon, *Chem. Rev.*, 1998, **98**, 637-674.
2 R. A. Dwek, *Chem. Rev.*, 1996, **96**, 683-720.
3 J. D. Marth and P. K. Grewal, *Nat. Rev. Immunol.*, 2008, **8**, 874-887.
4 G. A. Rabinovich and M. A. Toscano, *Nat. Rev. Immunol*., 2009, **9**, 338-352.
5 W. I. Weis and K. Drickamer, *Annu. Rev. Biochem.*, 1996, **65**, 441-473.
6 M. Mammen, S.-K. Choi and G. M. Whitesides, *Angew. Chem. Int. Ed*., 1998, **37**, 2754-2794.
7 J. J. Lundquist and E. J. Toone, *Chem. Rev.*, 2002, **102**, 555-578.
8 Y. C. Lee and R. T. Lee, *Acc. Chem. Res*., 1995, **28**, 321-327.
9 L. L. Kiessling, J. E. Gestwicki and L. E. Strong, *Angew Chem Int Ed*., 2006, **45**, 2348-2368.
10 N. Jayaraman, *Chem. Soc. Rev.*, 2009, **38**, 3463-3483.
11 C. Fasting, C. A. Schalley, M. Weber, O. Seitz, S. Hecht, B. Koksch, J. Dernedde, C. Graf, E.-W. Knapp and R. Hag, *Angew Chem Int Ed*., 2012, **51**, 10472-10498.
12 T. Feizi and W. Chai, *Nat. Rev. Mol. Cell Biol.*, 2004, **5**, 582-588.
13 T. Horlacher and P. H. Seeberger, *Chem. Soc. Rev.*, 2008, **37**, 1414-1422.
14 P.-H. Liang, C.-Y. Wu, W. A. Greenberg and C.-H. Wong, *Curr. Opin. Chem. Biol.*, 2008, **12**, 86-92.
15 N. Laurent, J. Voglmeir and S. L. Flitsch, *Chem. Commun.*, 2008, 4400-4412.
16 S. Park, J. C. Gildersleeve, O. Blixt and I. Shin, *Chem. Soc. Rev.*, 2013, **42**, 4310-4326.
17 J. M. de la Fuente, A. G. Barrientos, T. C. Rojas, J. Rojo, J. Cañada, A. Fernández and S. Penadés, *Angew. Chem. Int. Ed.*, 2001, **40**, 2258-2261.
18 H. Otsuka, Y. Akiyama, Y. Nagasaki and K. Kataoka, *J. Am. Chem. Soc.*, 2001, **123**, 8226-8230.
19 J. M. de la Fuente and S. Penadés, *Biochim. Biophys. Acta, Gen. Subj.*, 2006, **1760**, 636–651.
20 K. El-Boubbou and X. Huang, *Curr. Med. Chem.*, 2011, **18**, 2060-2078.
21 Z. Liu,Y. Jiao, Y. Wang, C. Zhou and Z. Zhang, *Adv. Drug Deliv. Rev.*, 2008, **60**, 1650-1663.
22 C.-C. Lin, Y.-C. Yeh, C.-Y. Yang, G.-F. Chen, Y.-C. Chen, Y.-C. Wu and C.-C. Chen, *Chem. Commun.*, 2003, **23**, 2920-2921.
23 X. Wang, O. Ramström, and M. Yan, *Analyst*, 2011, **136**, 4174-4178.
24 E. Mahn, T. Aastrup and M. Barboiu, *Chem. Commun.*, 2010, **46**, 5491-5493.
25 X. Wang, E. Matei, A. M. Gronenborn, O. Ramström and M. Yan, *Anal. Chem.*, 2012, **84**, 4248-4252.

26 C.-H. Liang, C.-C. Wang, Y.-C. Lin, C.-H. Chen, C.-H. Wong and C.-Y. Yu, *Anal. Chem.*, 2009, **81**, 7750-7756.

27 X. Wang, O. Ramström and M. Yan, *Anal. Chem.*, 2010, **82**, 9082-9089.

28 Y.-Y. Chien, M.-D. Jan, A. K. Adak, H.-C. Tzeng, Y.-P. Lin, Y.-J. Chen, K.-T. Wang, C.-T. Chen, C.-C. Chen and C.-C. Lin, *ChemBioChem*, 2008, **9**, 1100-1109.

29 A. A. Kulkarni, C. Fuller, H. Korman, A. A. Weiss and S. Iyer, *Bioconjugate Chem.*, 2010**, 21**, 1486-1493.

30 C. L. Schofield, B. Mukhopadhyay, S. M. Hardy, M. B. McDonnell, R. A. Field and D. A. Russell, *Analyst*, 2008, **133**, 626-634.

31 C. L. Schofield, R. A. Field and D. A. Russell, *Anal. Chem.*, 2007, **79**, 1356-1361.

32 M. J. Martin, A. Rashid, M. Rejzek, S. A. Fiarhurst, S. A. Wharton, S. R. Martin, J. W. McCauley, T. Wileman, R. A. Field and D. A. Russell, *Org. Biomol. Chem.*, 2013, **11**, 7101-7107.

33 M. Marradi, F. Chiodo, I Garcia and S. Penadés, *Chem. Soc. Rev.*, 2013, **42**, 4728-4745.

34 Q. Tong, X. Wang, H. Wang, T. Kubo and M. Yan, *Anal. Chem.*, 2012, **84**, 3049-3052.

35 R. Freeman and I. Willner, *Chem. Soc. Rev.*, 2012, **41**, 4067-4085.

35 Y. Chen, T. Ji and Z. Rosenzeig, *Nano Lett.*, 2003, **3**, 581-584.

37 X.-L. Sun, W. Cui, C. Haller and E. L. Chaikof, *ChemBioChem*, 2004, **5**, 1593-1596.

38 J. M. de la Fuente and S. Penadés, *Tetrahedron Asymm.*, 2005, **16**, 387-391.

39 Z. Dai, A. N. Kawde, Y. Xiang, J. T. Belle, J. La Gerlach, V. P. Bhavanandan, I. Joshi and J. Wang, *J. Am. Chem. Soc.*, 2006, **128**, 10018-10019.

40 P. Babu, S. Sinha and A. Surolia, *Bioconjugate Chem.*, 2007, **18**, 146-151.

41 R. J. Pieters, *Org. Bimol. Chem.*, 2009, **7**, 2013-2025.

42 S. I. van Kasteren, S. J. Campbell, S. Serres, D. C. Anthony, N. Sibson and B. G. Davis, *Proc. Natl. Acad. Sci.*, 2009, **106**, 18-23.

43 K. El-Boubbou, D. C. Zhu, C. Vasileiuo, B. Borhan, D. Prosperi, W. Li and X. Huang, *J. Am. Chem. Soc.*, 2010, **132**, 4490-4499.

44 L. Lartigue, C. Innocenti, T. Kalavani, A. Awwad, M. Sanchez Duque, Y. Guari, J. Larionova, C. Guerin, J.-L. Georges, D. Gatteschi and C. Sangregorio, *J. Am. Chem. Soc.*, 2011, **133**, 10459-10472.

45 M. Marradi, D. Alcantara, J. M. de la Fuente, M. L. Garcia-Martin, S. Cerdan and S. Penadés, *Chem. Commun.*, 2009, 3922-3924.46 J. Gallo, I. Garcia, D. Padro, B. Arnaiz and S. Penadés, *J. Mater. Chem.*, 2010, **20**, 10010-10020.

47 J. Frigell, I. Garcia, V. Gomez-Vallejo, J. Liop and S. Penadés, *J. Am. Chem. Soc.*, 2014, **136**, 449-457.

48 T. D. Farr, C.-H. Lai, D. Grunstein, Guillermo, Orts-Gil, C.-C. Wang, P. Boehm-Sturm, P. H. Seeberger and C. Harms, *Nano Letts*, **14**, 2130-2134.

49 C.-H. Lai, C.-Y. Lin, H.-T. Wu, H.-S. Chan, Y.-J. Chuang, C.-T. Chen and C.-C. Lin, *Adv. Funct. Mater.*, 2010, **20**, 3948-3958.

50 A. Robinson, J.-M. Fang, P.-T. Chou, K.-W. Liao, R.-M. Chu and S.-J. Lee, *ChemBioChem*, 2005, **6**, 1899-1905.

51C.-T. Chen, Y. S. Munot, S. B. Salunke, Y.-C. Wang, R.-K. Lin, C.-C. Lin, C.-C. Chen and Y.-H. Liu, *Adv. Funct. Mater.,* 2008, **18**, 527-540.

52 Y. Higuchi, M. Oka, S. Kawakami and M. Hashida, *J. Control. Rel.*, 2008, **125**, 131-136.

53 R. Kikkeri, B. Lepenies, A. Adibekian, P. Laurino and P. H. Seeberger, *J. Am. Chem. Soc.*, 2009, **131**, 2110-2112.

54 T. Ohyanagi, N. Nagahori, K. Shimawaki, H. Hino, T. Yamashita, A. Sasaki, T. Jin, T. Iwanaga, M. Kinjo and S.-I. Nishimura, *J. Am. Chem. Soc.*, 2011, **133**, 12507-12517.

55 T. L. Doane and C. Burda, *Chem. Soc. Rev.*, 2012, **41**, 2885-2911.

56 J. D. Gibson, B. P. Khanal and E. R. Zubarev, *J. Am. Chem. Soc.*, 2007, **129**, 11653-11661.

57 J. R. Hwu, Y.-S. Lin, T. Josephrajan, M.-H. Hsu, F.-Y. Cheng, C.-S. Yeh, W.-C. Su and D.-B. Shieh, *J. Am. Chem. Soc.*, 2009, **131**, 66-68.

58 C.-H. Lai, T.-C. Chang, Y.-J. Chuang, D.-L. Tzou and C.-C. Lin, *Bioconjugate Chem.*, 2013, **24**, 1698-1709.

59 A. Aykac, M. C. Martos-Maldonado, J. M. Casa-Solvas, I. Quesada-Soriano, F. Garcia-Maroto, L. Garcia-Fuentes and A. Vargas-Berenguel, *Langmuir*, 2014, **30**, 234-242.

60 R. F. Barth, J. A. Coderre, M. G. M. Vicente and T. E. Blue, *Clin. Cancer Res.*, 2005, **11**, 3987-4002.

61 C.-H. Lai, Y.-C. Lin, F.-I. Chou, C.-F. Liang, E.-W. Lin, Y.-J. Chuang and C.-C. Lin, *Chem. Commun.*, 2012, **48**, 612-614.

62 C.-H. Lai, N.-C. Lai, Y.-J. Chuang, F.-I. Chou, C.-M. Yang and C.-C. Lin, *Nanoscale*, 2013, **5**, 9412-9418.

63 P. K. Jain, X. Huang, I. H. Ei-Sayed and S. H. Ei-Sayed, *Acc. Chem. Res.*, 2008, **41**, 1578-1586.

64 K. Saha, S. S. Agasti, C. Kim, X. Li and V. M. Rotello, *Chem. Rev.*, 2012, **112**, 2739-2779.

65 Y. Choi, N.-H. Ho and C.-H. Tung, *Angew. Chem. Int. Ed.*, 2007, **46**, 707-709.

66 C. Guarise, L. Pasquato, V. De Filippis and P. Scrimin, *Proc. Natl. Acad. Sci. U. S. A.*, 2006, **103**, 3978-3982.

67 S. Gupta, H. Andresen and M. M. Stevens, *Chem. Commun.*, 2011, **47**, 2249-2251.

68 C.-C. Yu, L.-D. Huang, D. H. Kwan, W. W. Wakarchuk, S. G. Withers and C.-C. Lin, *Chem. Commun.*, 2013, **49**, 10166-10168.

69 C.-C. Lin, Y.-C. Yeh, C.-Y. Yang, C.-L. Chen, G.-F. Chen, C.-C. Chen and Y.-C. Wu, *J. Am. Chem. Soc.*, 2002, **124**, 3508-3509.

70 I. Papp, C. Sieben, K. Ludwig, M. Roskamp, C. Bottcher, S. Schlecht, A. Herrmann and R. Haag, *Small*, 2010, **24**, 2900-2906.

71 K. El-Boubbou, C. Gruden and X. Huang, *J. Am. Chem. Soc.*, 2007, **129**, 13392-13393.

72 L. H. Liu, H. Dietsch, P. Schurtenberger and M. Yan, *Bioconjugate Chem.*, 2009, **20**, 1349-1355.

73 P.-C. Lin, C.-C. Yu, H.-T. Wu, Y.-W. Lu, C.-L. Han, A.-K. Su, Y.-J. Chen and C.-C. Lin, *Biomacromolecules*, 2013, **14**, 160-168.

74 B. Mukhopadhyay, M. Martins, R. Karamanska, D. A. Russell and R. A. Field, *Tetrahedron Lett.*, 2009, **50**, 886-889.

75 N. P. Pera, A. Kouki, S. Haataja, H. M. Branderhorst, R. M. J. Liskamp, G. M. Visser, J. Finne and R. J. Pieters, *Org. Biomol. Chem.*, 2010, **8**, 2425-2429.

76 M. Hartmann, P. Betz, Y. Sun, S. N. Gorb, T. K. Lindhorst and A. Krueger, *Chem. Eur. J.*, 2012, **18**, 6485-6492.

77 M. Reynolds, M. Marradi, A. Imberty, S. Penadés and S. Perez, *Chem. Eur. J.*, 2012, **18**, 4264-4273.

78 O. Martinez-Avila, K. Hijazi, M. Marradi, C. Clave, C. Campion, C. Kelly and S. Penadés, *Chem. Eur. J.*, 2009, **15**, 9874-9888.

79 B. Arnaiz, O. Martinez-Avila, J. M. Falcon-Perez and S. Penadés, *Bioconjugate Chem.*, 2010, **23**, 814-825.

80 F. Chiodo, M. Marradi, J. Park, A. F. J. Ram, S. Penades, I. van Die and B. Tefsen, *ACS Chem. Biol*., 2014, **9**, 383-389.

81 M. D. Disney and P. H. Seeberger, *Chem. Biol.* 2004, **11**, 1701-1707.

82 M. D. Disney, J. Zheng, T. M. Swager and P. H. Seeberger, *J. Am. Chem. Soc.*, 2004, **126**, 13343-13346.

83 P. Laurino, R. Kikkeri, N. Azzouz and P. H. Seeberger, *NanoLett*, 2011, **11**, 73-78.

84 A. K. Adak, A. P. Leonov, N. Ding, T. Jyothi, S. Kularatne, P. S. Low and A. Wei, *Bioconjugate Chem*., 2010, 21, 2065-2075.

85 A. K. Adak, W. J. Boley, D. P. Lyvers, G. T. Chiu, R. Reifenberger, P. S. Low and A. Wei, *ACS Appl. Mater. Interfaces*, 2013, **5**, 6404-6411.

A brief biography of authors

Avijit K Adak obtained his Ph.D. in organic chemistry (2004) from the BESU (*presently* IIEST, Shibpur), India, with Prof. S. P. Goswami. In 2005, he took a postdoctoral position with Prof. Chun-Cheng Lin at the Academia Sinica and National Tsing Hua University, Taiwan, where he investigated glyconanoparticles as scaffolds for carbohydrate-mediated interactions. In 2008, he moved to Purdue University, USA, where he worked with Prof. Alexander Wei on the synthesis of oligosaccharides and their glycoconjugates and on label-free methods for bacterial pathogen detection. Currently, he is working with Prof. Chun-Cheng Lin at the National Tsing Hua University, Taiwan, where he is developing oriented and covalent protein microarrays.

Hong-Jyune Lin obtained her B.S. in Chemistry from the National Taiwan Normal University in 2008. In the same year, she began her journey into the world of carbohydrate chemistry, and she received her Master's degree from the National Tsing Hua University in 2010. She continued her education as a Ph.D. student majoring in Organic Chemistry at the same school. The main focus of her research is on the methodology exploitation of synthesizing new types of glycolipids. Currently, she is working toward her doctoral degree under the supervision of Prof. Chun-Cheng Lin.

Chun-Cheng Lin studied chemistry at the National Tsing Hua University and National Taiwan University (B.S. 1987 and M.S. 1989). He joined the group of Prof. Chi-Huey Wong (The Scripps Research Institute) and received his Ph.D. in 1997. After a postdoctoral stay of one year at the same laboratory, he started his independent research at Academia Sinica in 1998. In 2006, he moved to National Tsing Hua University and was promoted to full professor in 2007. His research interests cover carbohydrate synthesis, microarray fabrication, protein conjugation, and nanotechnology.

TOC

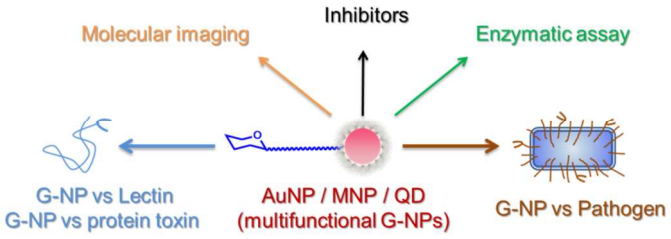

Glyconanoparticles decorated with multiple copies of various biologically relevant carbohydrates serve as scaffolds for protein binding assay, molecular imaging, targeted therapy, and bacterium detection.